UNCLASSIFIED

AD NUMBER

AD305684

CLASSIFICATION CHANGES

TO: unclassified

FROM: confidential

LIMITATION CHANGES

TO:

Approved for public release, distribution unlimited

FROM:

Availability: Document partially illegible.

AUTHORITY

NRL ltr 7103/136, 19 Nov 96; NRL ltr 7103/136, 19 Nov 96

THIS PAGE IS UNCLASSIFIED

AD-305 684

EVALUATION OF EFFECTS OF ELEMENT INTERACTIONS IN A LARGE LOW-FREQUENCY ARRAY

[UNCLASSIFIED TITLE]

Roland V. Baier

Transducer Branch
Sound Division

February 10, 1959

U. S. NAVAL RESEARCH LABORATORY
Washington, D.C.

7 10 2 51

CONFIDENTIAL

SECURITY

CONTENTS

ABSTRACT
[Confidential]

Mutual interactions between elements of a transducer array affect the velocities, radiation loading, and beam patterns which are obtained in a given array and unit design. These effects are of particular interest for transducer arrays which have relatively large inactive areas interspersed in the radiating surface. These interaction effects have been evaluated from theoretical expressions in a manner which takes account of the array geometry, the electromechanical properties of the array elements, and the phase and magnitude of the electrical excitation of a 44-unit 1-kc planar array.

The results of the computations are presented as the theoretical velocities, radiation loading, input impedance, power in, power out, and the efficiencies which are effective for the individual elements in the array within the assumptions made in the theory. These results are presented for several degrees of electrically steering of the principal lobe. Plots of the beam patterns are presented for various amounts of electrical steering of the principal lobe and are compared with the situation which would result if the interaction effects were neglected.

Some of the more interesting observations are the following. The outer radiators of the array have the greater real part of the radiation load, the smaller velocities, and the better efficiencies. The behavior of the individual radiators in the array as the major lobe is steered away from the broadside position reveals a decrease in the velocities, an increase in the radiation load, and a small gain in the conversion efficiency. For the array as a whole, both the power into and the power out of the array decrease but the conversion efficiency (as determined from the ratio of the total acoustic power delivered by the array to the total electrical power into the array) increases as the major lobe is steered away from the principal axis of the array. The effective source level of the array is reduced as the major lobe is steered. The fact that the array is more efficient (minimum value 58.8 percent) when the interactions are included as compared with 55.8-percent efficiency when interactions are neglected completely has not been explained thus far.

PROBLEM STATUS

This is an interim report on the problem; work is continuing.

AUTHORIZATION

EVALUATION OF EFFECTS OF ELEMENT INTERACTIONS
IN A LARGE LOW-FREQUENCY ARRAY
[Unclassified Title]

INTRODUCTION

The Naval Research Laboratory is engaged in an ASW program which involves a systematic study of sonar detection systems at successively lower frequencies. The major interest, for the last few years, has been in 1-kc system now in the process of fabrication at NRL. In order to satisfy the directional requirements for target location at this low frequency, sonar projectors become rather large in physical size and weight. One method that is generally employed for reducing the overall weight for a given power density in the beam, while maintaining the desired directionality for these low frequencies, is to space the individual radiators as far apart as is permissible. A more thorough analysis is required to evaluate the effects of inactive areas in the radiating surface on the performance of the array as a sonar projector and receiver, particularly with respect to the interactions between the individual radiators of the array. This analysis involves the computation of the mutual acoustic immobility* between the various possible pairs of radiators in the array.

Generally, in computing radiation loading, the assumption is made that the velocities of the radiators are all equal when excited by the same force, at least for arrays which contain more than a few identical radiators. This is a satisfactory assumption if each radiator is independent of every other radiator and feels only the load presented by the acoustic medium reaction. This report introduces, in addition to the acoustic medium reaction, a reaction due to the pressure of all other radiators in the field. Thus, one radiator produces a pressure in the region occupied by another radiator, so that the second radiator must work against both the acoustic medium reaction and the pressure produced by the first radiator. In an array of radiators, each radiator must work against the acoustic medium reaction and the sum of the pressures resulting from all other array radiators. This interaction of one radiator with another is the source of the mutual acoustic immobility.

THEORY OF MUTUAL MECHANICAL IMMOBILITY

A mathematical expression for the mutual mechanical immobility between two identical circular pistons vibrating in the plane of an infinite rigid baffle has been developed by Pritchard.† This expression forms the basic starting point for the treatment hereafter discussed. If the radius of the individual piston is a, and the separation between centers of the pistons is d (Fig. 1), the mutual immobility Y_{12} given by Pritchard for $d>2a$ is

$$Y_{12} = G_{12} + j\, B_{12} = \rho c\, \pi a^2 \sum_{s=0}^{\infty} \left(\frac{a}{d}\right)^s \sigma_s(ka)\, \xi_s\,(kd) \tag{1}$$

---

*See Appendix A.

†R.L. Pritchard, "Directivity of Acoustic Linear Point Arrays," Harvard Univ., Acoustics Research Laboratory Tech. Memo. No. 21 (Unclassified), N5 ori 76 T.O.10, Jan. 15, 1951, Appendix C
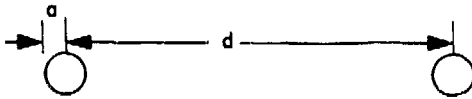
Fig. 1 - Geometry of two identical circular pistons

where

ρ = density of the medium (gm/cm^3)

c = velocity of sound in the medium (cm/sec)

ρc = characteristic immobility of the medium

$$c_s(ka) = 2 \sum_{m+n=s} \frac{\Gamma(m + n + \frac{1}{2})}{\sqrt{\pi}\, m!\; n!} J_{m+1}(ka)\, J_{n+1}(ka)$$

$$\xi_s(kd) = \sqrt{\frac{\pi}{2kd}} \left[J_{s+\frac{1}{2}}(kd) + j(-1)^s J_{-s-\frac{1}{2}}(kd) \right]$$

$$k = 2\pi/\lambda$$

in which

Γ = gamma function

J = Bessel function

λ = wavelength of sound in the medium.

Figure 2 gives a plot of the real and imaginary parts of Y_{12} versus the separation between the two pistons and illustrates the oscillatory behavior of this function. The curves of Fig. 2 apply to the cases where $ka = 1.1167$ and $ka = 1.5819$ and give both the real and imaginary parts of the radiation immobilities for all values of separation of the two pistons which lie between $kd = \pi$ and $kd = 33$. The curves are plotted in dimensionless form so that it is necessary to multiply the ordinate by $\rho c \pi a^2$ in order to obtain the actual value in the correct units.

To indicate the general procedure of how one may include the effects of interaction between various radiators, one begins with two identical circular pistons. The net radiation force on the first piston is given by

$$f_1 = Y_{11} V_1 + Y_{12} V_2 \tag{2}$$

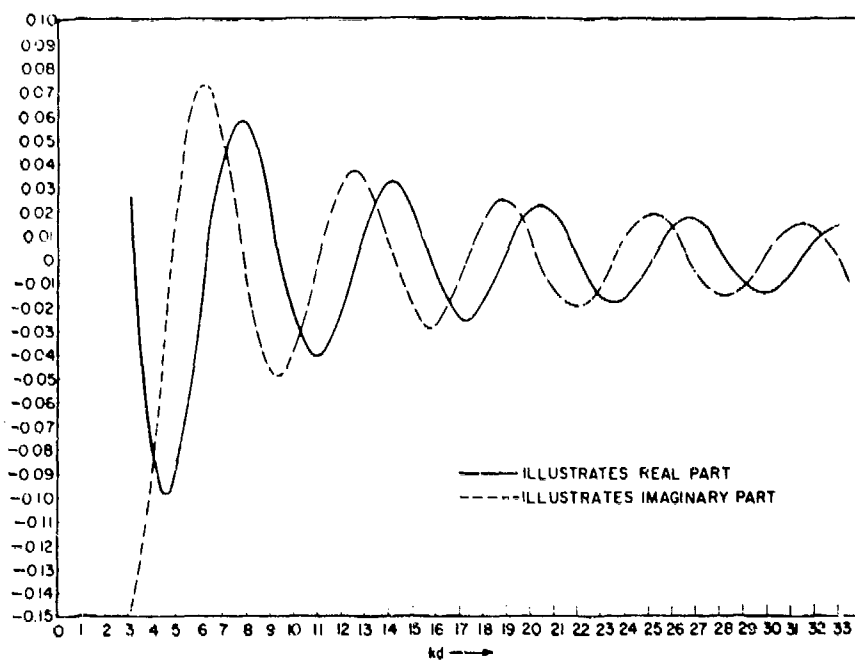and for the second piston

$$f_2 = Y_{21} V_1 + Y_{22} V_2 \tag{3}$$

Fig. 2a – Mutual immobility between two circular pistons in an
infinite rigid baffle for ka = 1.1167
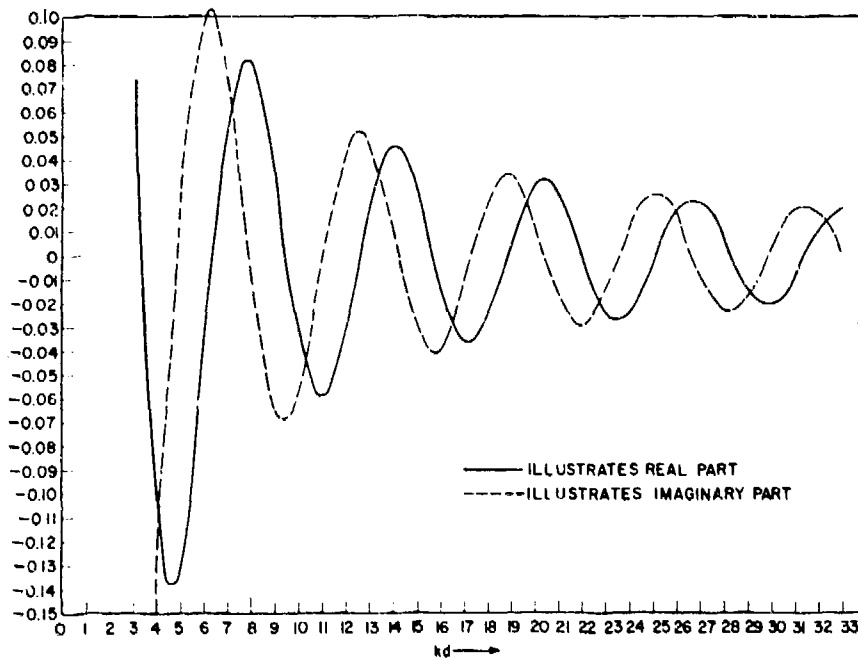

Fig. 2b – Mutual immobility between two circular pistons in an
infinite rigid baffle for ka = 1.589

where Y_{11} is the self-radiation immobility, which is associated with a single piston in the absence of all other acoustic sources and scatterers, V_1 is the velocity of the first piston, and V_2 is the velocity of the second piston.

Since distance from piston one to piston two is the same as from two to one, $Y_{12} = Y_{21}$ from Eq. (1), and since the two pistons are identical, $Y_{11} = Y_{22}$. The net radiation immobility is defined as the net radiation force divided by the velocity of the element; therefore, for piston one, the net radiation immobility is given by

$$Y_1 = \frac{f_1}{V_1} = Y_{11} + Y_{12} \frac{V_2}{V_1} \tag{4}$$

and the net radiation immobility for piston two is

$$Y_2 = \frac{f_2}{V_2} = Y_{11} + Y_{12} \frac{V_1}{V_2} \; . \tag{5}$$

If there are more than one pair of pistons, then each pair will be considered independently as a first approximation and the net radiation immobility is given by extending the above equations to include the additional radiators.

It is noted that the symbols Y_{11} and Y_{12} have been employed for the radiation immobility. This symbolism is based upon the mobility analogy where one chooses force analogous to current and velocity analogous to voltage. Since this paper is concerned only with magnetic-field-type transducers, where the force developed is proportional to the current, it is convenient to use immobility quantities for the mechanical components of the transducer.

APPLICATION OF THE THEORY TO A
THREE-ELEMENT ARRAY

In order to illustrate how one includes the interaction effects in an array of radiators, the ideas developed above are applied to an array in which it is possible to have more than one unique array element velocity, even if identical elements and identical excitation are employed. As an elementary example, let this array consist of three identical radiators which are equally spaced along a straight line, as shown in Fig. 3. These elements are considered to be magnetic devices, each of which is representable by an equivalent circuit as shown in Fig. 4.
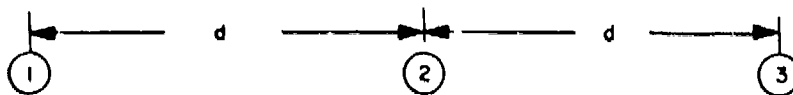
Fig. 3 - Array of three identical radiators
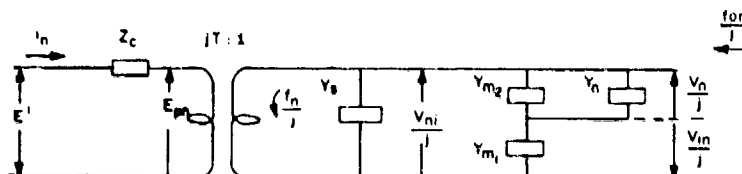
Fig. 4 - Equivalent circuit of a single XEM-3B transducer element (see Appendix A for definitions of the terms)

Equations for a Single Element

The equations which describe the behavior of one element are

$$V_{ni} = V_n - V_{in} \tag{6}$$

$$E' = Z_c\, i_n + T\, V_{ni} \tag{7a}$$

$$f_{on} = f_n + \left(Y_{m_2} + Y_n\right) V_n + Y_s\, (V_n - V_{in}) \tag{7b}$$

$$f_n = Y_{\cdot_1}\, V_{in} + Y_s\, (V_{in} - V_n) = -Ti_n \;. \tag{7c}$$

Since the only acoustic sources assumed in this problem are those associated with the mutual immobility, the force f_o is neglected.

By combining Eqs. (7b) and (7c), one finds that

$$V_n = \frac{-Y_{m_1}}{Y_{m_2} + Y_n}\, V_{in} \;. \tag{8}$$

The properties of the equivalent transformer are

$$E_{pn} = T\, V_{ni} \; ; \; f_n = -Ti_n \;. \tag{9}$$

Rewriting Eq. (7a) using (6), (8), and (9), one obtains

$$\frac{E'T}{Z_c} = Ti_n + \frac{T^2}{Z_c} \left(\frac{Y_{m_1} + Y_{m_2} + Y_n}{Y_{m_1}} \right) V_n .$$ (10)

Equation (7c) may be written as

$$Ti_n = \left[Y_n \left(Y_s + Y_{m_1} \right) + Y_s \left(Y_{m_1} + Y_{m_2} \right) + Y_{m_1} Y_{m_2} \right] \frac{V_n}{Y_{m_1}} .$$ (11)

Elimination of the primary current between Eqs. (10) and (11) gives

$$\frac{E'T}{Z_c} = \left[Y_n \left(Y_{m_1} + Y_s + \frac{T^2}{Z_c} \right) + \left(Y_{m_1} + Y_{m_2} \right) \left(\frac{T^2}{Z_c} + Y_s \right) + Y_{m_1} Y_{m_2} \right] \frac{V_n}{Y_{m_1}} .$$ (12)

Now if the condition that the transducer be driven at its mechanical resonance in air is imposed, which condition is defined as

$$Y_{m_1} Y_{m_2} + j \left(Y_{m_1} + Y_{m_2} \right) B_s = 0$$

then Eq. (12) reduces to

$$\frac{E'T}{Z_c} = \left[Y_n \left(Y_{m_1} + Y_s \quad \frac{T^2}{Z_c} \right) + \left(Y_{m_1} + Y_{m_2} \right) \left(\frac{T^2}{Z_c} + G_s \right) \right] \frac{V_n}{Y_{m_1}} .$$ (13)

These equations apply to a single XEM-3B transducer (i.e., a single element, the nth element). The particular problem which has been chosen for evaluation requires that each unit radiator for the array shall contain not one but four of the elements represented in Fig. 4, which are connected together electrically so that a common current flows through each of the primaries (i.e., in series electrically). For the four elements in series, Eq. (7a) then gives E = 4E' (voltages add), so that Eq. (13) becomes, for a unit radiator

$$\frac{E T}{Z_c} = 4 \left[Y_n \left(Y_{m_1} + Y_s + \frac{T^2}{Z_c} \right) + \left(Y_{m_1} + Y_{m_2} \right) \left(\frac{T^2}{Z_c} + G_s \right) \right] \frac{V_n}{Y_{m_1}} .$$ (14)

Elements in Parallel Electrically

One must now determine the various velocities and forces which exist in the three-unit array. The distribution of velocities and forces will depend upon how the three radiators are interconnected electrically. First, consider the case where the three radiators are connected in parallel. This means that each radiator has the same voltage E applied at the electric terminals. Then by changing E' to $E/4$ to account for the fact that each unit radiator contains four identical series-connected elements and successively allowing the subscript n to assume the values 1, 2, and 3 in Eq. (7a) one gets the following set of three equations:

$$\frac{F}{4} = Z_c\, i_1 + T\, V_{1i}$$

$$\frac{E}{4} = Z_c\, i_2 + T\, V_{2i}$$

$$\frac{E}{4} = Z_c\, i_3 + T\, V_{3i}\;.$$

The equations which apply to the mechanical side of the three radiators, assuming $f_o = 0$, are obtained Eq. (7b) by running the subscript n from 1 through 3 and are

$$-f_1 = \left(Y_{m_2} + Y_1\right) V_1 + Y_s\, V_{1i}$$

$$-f_2 = \left(Y_{m_2} + Y_2\right) V_2 + Y_s\, V_{2i}$$

$$-f_3 = \left(Y_{m_2} + Y_3\right) V_3 + Y_s\, V_{3i}\;,$$

Substitution of Eqs. (8) and (9) and appropriate expressions similar to Eqs. (4) and (5) into the above sets of equations and elimination of the currents and forces between the equations gives the desired answer. The set of three equations which define the relationships between <u>velocities</u>, <u>mutual immobilities</u>, and the common <u>source voltage</u> are given below:

$$\frac{E\,T}{Z_c} \frac{Y_{m_1}}{Y_{m_1} + Y_s + \dfrac{T^2}{Z_c}} = 4\, V_1 \left[\frac{\left(Y_{m_1} + Y_{m_2}\right)\left(G_s + \dfrac{T^2}{Z_c}\right)}{Y_{m_1} + Y_s + \dfrac{T^2}{Z_c}} + Y_{11} \right] + 4\, Y_{12}\, V_2 + 4\, Y_{13}\, V_3 \qquad (15a)$$

$$\frac{E\,T}{Z_c} \frac{Y_{m_1}}{Y_{m_1} + Y_s + \dfrac{T^2}{Z_c}} = 4\, Y_{12}\, V_1 + 4\, V_2 \left[\frac{\left(Y_{m_1} + Y_{m_2}\right)\left(G_s + \dfrac{T^2}{Z_c}\right)}{Y_{m_1} + Y_s + \dfrac{T^2}{Z_c}} + Y_{11} \right] + 4\, Y_{23}\, V_3 \qquad (15b)$$

$$\frac{E\,T}{Z_c}\,\frac{Y_{m_1}}{Y_{m_1} + Y_s + \dfrac{T^2}{Z_c}} = 4\,Y_{13}\,V_1 + 4\,Y_{23}\,V_2 + 4\,V_3\left[\frac{\left(Y_{m_1} + Y_{m_2}\right)\left(G_s + \dfrac{T^2}{Z_c}\right)}{Y_{m_1} + Y_s + \dfrac{T^2}{Z_c}} + Y_{11}\right]. \quad (15c)$$

These three equations are complex-variable equations and therefore represent six equations in real variables. Both the real and imaginary parts of the three complex velocities can be evaluated if E is specified. If one carries out the solution of these equations, it is possible to show that $V_1 = V_3$ (both magnitude and phase) but $V_1 \neq V_2$. It is further noted that Z_c, the clamped electrical impedance, appears in the equations and consequently must affect the various velocities and velocity ratios.

Elements in Series Electrically

Now suppose that one uses the same array but connects the three radiators in series, that is, with all radiators having a common current in the primary. This means that each radiator is driven by the same mechanical force f. Then Eq. (7b) may again be used by removing the subscript n on f and running the other n subscripts to 3 to obtain

$$-f = \left(Y_{m_2} + Y_1\right) V_1 + Y_s\,V_{1i} \quad\quad\quad\quad (16a)$$

$$-f = \left(Y_{m_2} + Y_2\right) V_2 + Y_s\,V_{2i} \quad\quad\quad\quad (16b)$$

$$-f = \left(Y_{m_2} + Y_3\right) V_3 + Y_s\,V_{3i}\;. \quad\quad\quad\quad (16c)$$

Combining Eqs. (6) and (7c), one gets

$$-f = \left(Y_s + Y_{r_1}\right) V_{ni} - Y_{m_1}\,V_n$$

where n assumes the values 1, 2, and 3. Eliminating V_{ni} between these last two sets of equations, the following three equations are obtained after substitution of the proper net radiation immobilities:

$$\frac{Y_{m_1}}{Y_{m_1} + Y_s}\,f = \left[\frac{Y_s\left(Y_{m_1} + Y_{m_2}\right) + Y_{m_1}\,Y_{m_2}}{Y_s + Y_{m_1}} + Y_{11}\right]V_1 + Y_{12}\,V_2 + Y_{13}\,V_3 \quad (17a)$$

$$\frac{Y_{m_1}}{Y_{m_1} + Y_s}\,f = Y_{12}\,V_1 + \left[\frac{Y_s\left(Y_{m_1} + Y_{m_2}\right) + Y_{m_1}\,Y_{m_2}}{Y_3 + Y_{m_1}} + Y_{11}\right]V_2 + Y_{23}\,V_3 \quad (17b)$$

$$\frac{Y_{m_1}}{Y_{m_1} + Y_s} f = Y_{13} V_1 + Y_{23} V_2 + \left[\frac{Y_s \left(Y_{m_1} + Y_{m_2} \right) + Y_{m_1} Y_{m_2}}{Y_s + Y_{m_1}} + Y_{11} \right] V_3 \quad . \tag{17c}$$

One again obtains three complex-variable equations which represent six equations in real variables. It is again possible to show that $V_1 = V_3$ but $V_1 \neq V_2$.

One may note in contrast to the parallel connection the the ratio of velocities for the series connection is independent of the electrical properties of the radiators in the sense that the clamped electrical impedance does not appear in the equations. One can deduce from considerations such as those discussed above the following useful rule: For each and every geometrically and excitationally distinct symmetry position in an array of like elements, there is a corresponding unique velocity associated with the elements in that symmetry position.

BASIC ASSUMPTIONS OF THE THEORY

Certain assumptions have been made in the application of the foregoing techniques to three or more elements. These assumptions have been made in order to reduce the mathematical complexity of the problem and are as follows:

1. The expression derived by Pritchard for the interaction between two circular pistons in an infinite stiff baffle is an adequate first approximation to the interaction between two similar rectangular pistons having the same volume velocity but with an absence of baffles of any kind.

2. The shape of the velocity distribution over the surface of any given radiator is not altered by the pressures produced by other radiators which are interacting (that is, a linear addition of effects rather than a nonlinear perturbation computation is acceptable).

3. Neglecting those effects which are similar to diffraction phenomena for the first-order solutions is acceptable. (This assumption cannot be expected to be too valid for beam patterns at angles close to 90 degrees from the broadside principal axis.)

4. The transducing elements are linear devices.

5. All elements are mathematically identical.

RESULTS FOR A COMPLETE 44-UNIT ARRAY

Figure 5 is a schematic scaled illustration of the 44-unit array for which computations have been made. Each rectangle is a unit composed of four transducer elements electrically connected in series. All 44 units of the array are effectively connected in parallel. Figure 5 shows that there is a large portion of the array area which is inactive. The theoretical development is an evaluation of what effects these large inactive areas have on such transducer parameters as beam patterns, radiation loading, and electrical impedance changes associated with electrical steering.
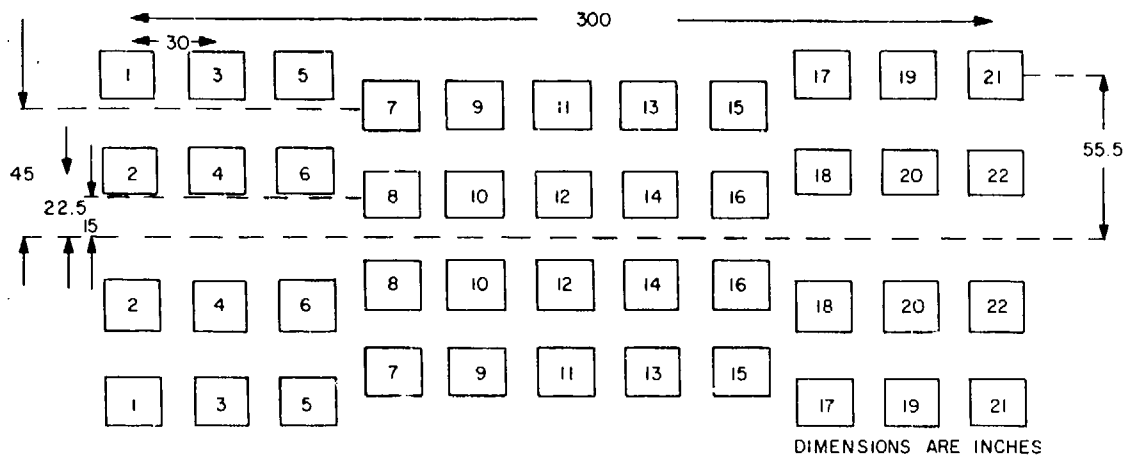
Fig. 5 - XEM-3B 1-kc array of 176 elements

Application of the symmetry rule for the unsteered array results in 12 unique velocities and net radiation immobilities. However, for electrical steering of the array in the long dimension of the array (or the horizontal plane) one gets 22 unique velocities and net radiation immobilities. (The symmetry positions are the mirror image positions with respect to the horizontal center line of the array.) Then for the steered array, 44 simultaneous equations in real variables must be solved for the 22 unknown velocities.

Table 1 gives the results of the Naval Research Laboratory Narec computations for the velocities of the radiators. The velocity is given in terms of the magnitude and phase angle where the excitation voltage (whose magnitude is 300 volts) is the phase reference. The odd numbered radiators are the outer radiators and the even numbered radiators are the inner radiators (Fig. 5). Comparing the outer radiators with the corresponding inner radiators, one observes that the inner radiators generally have the greater velocity. Another interesting comparison is the fact that for any given radiator the magnitude of the velocity usually decreases as the major lobe is electrically steered away from the broadside direction.

Table 2 gives the results of evaluation of equations similar to Eqs. (4) and (5) but extended to include terms for 22 velocities and gives the net radiation immobility for every unit in the array. Both the real part and the imaginary part of the net radiation immobility are listed for each situation of electrical steering of the main lobe. The immobilities are in dimensionless units which must be multiplied by ρcA, which is 3.7×10^8 gm/sec for this particular case. It is noted that generally the outer radiators have the larger radiation load and that corner elements have the greatest mass loading. For the case where interactions are neglected, the self-radiation load for a single unit is $0.506 + i0.673$ ρcA units. Therefore, one can see that at least for angles of beam steering less than 20 degrees the interactions reduce both the real and imaginary parts of the radiation load rather than increase the real part and reduce the imaginary part as might be expected.

Table 1
Radiator Velocity in Terms of Magnitude (cm/sec) and Phase Angle (degrees)
as a Function of the Angle of Steering of the Main Lobe

| Rad. No.*	0°		5°		10°		15°		20°		25°		30°	
	|V|	θ(V)	|V|	θ(V)	|V|	θ(V)	|V|	θ(V)	|V|	θ(V)	|V|	θ(V)	|V|	θ(V)
1	2.92	273.5	2.72	198.7	2.78	119.3	2.84	49.3	2.58	335.8	2.64	264.7	2.47	201.9
3	3.48	283.5	3.26	222.2	3.35	155.4	3.34	97.7	2.98	34.4	3.04	333.7	2.80	281.0
5	2.90	277.0	2.93	231.3	2.94	186.7	2.98	140.8	3.10	91.5	3.11	52.0	3.03	8.0
7	3.13	282.8	3.05	251.1	2.99	218.6	2.99	188.2	2.92	158.8	2.86	127.6	2.88	96.1
9	2.72	280.9	2.81	266.4	2.90	252.3	2.83	236.6	2.71	219.1	2.67	203.3	2.64	189.3
11	3.03	282.6	2.93	282.4	2.78	281.4	2.77	279.8	2.82	278.0	2.74	276.4	2.56	274.4
13	2.72	280.9	2.79	295.4	2.90	309.3	2.90	324.6	2.84	340.6	2.79	353.5	2.71	3.0
15	3.13	282.8	3.06	314.5	2.97	346.9	2.91	16.7	2.76	44.5	2.63	71.9	2.58	97.2
17	2.90	277.0	2.95	323.8	3.00	10.2	3.01	57.1	2.99	103.1	2.86	146.5	2.69	188.7
19	3.48	283.5	3.21	344.1	3.21	48.6	3.13	104.1	2.81	163.2	2.83	218.0	2.64	265.0
21	2.92	273.5	2.76	348.9	2.90	68.5	3.01	139.7	2.92	214.2	3.15	284.8	3.19	347.7
2	3.29	273.1	3.02	199.3	3.00	119.1	3.01	48.4	2.67	331.6	2.87	257.8	2.76	193.8
4	3.72	277.8	3.46	216.4	3.56	149.7	3.55	91.5	3.27	28.1	3.39	329.4	3.13	276.5
6	3.33	280.3	3.37	235.0	3.36	189.8	3.37	142.8	3.39	96.7	3.25	51.2	3.16	4.7
8	3.15	285.5	3.04	253.4	2.95	221.1	2.87	192.4	2.76	164.1	2.80	134.6	2.96	106.7
10	3.08	287.9	3.15	272.8	3.22	257.0	3.18	238.5	3.16	219.4	3.14	205.2	3.03	193.5
12	3.15	286.3	3.07	286.0	2.99	285.7	3.10	286.1	3.27	286.6	3.22	285.8	3.00	282.9
14	3.08	287.9	3.15	303.1	3.23	317.8	3.12	332.8	2.92	347.9	2.83	359.7	2.89	8.0
16	3.15	285.5	3.06	316.3	2.94	347.5	2.98	15.4	3.07	39.9	3.15	65.5	3.28	93.4
18	3.33	280.3	3.42	325.4	3.48	351.6	3.49	52.9	3.59	97.1	3.60	138.0	3.48	178.1
20	3.72	277.8	3.39	338.8	3.44	45.4	3.45	101.6	3.12	162.0	3.23	219.1	3.11	267.8
22	3.29	273.1	3.15	347.9	3.29	65.6	3.35	136.6	3.21	210.6	3.35	280.9	3.30	345.4

*See Fig. 5

Table 2
Radiator Net Radiation Immobility as a Function of the
Angle of Steering of the Main Lobe

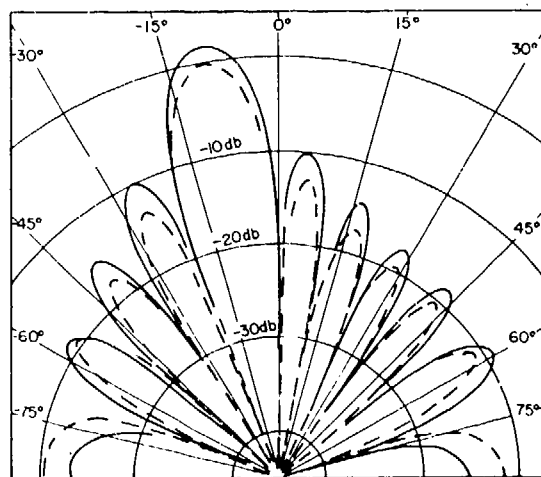| Rad. No.	0°		5°		10°		15°		20°		25°		30°	
	$\frac{G}{\rho cA}$	$\frac{B}{\rho cA}$	$\frac{G}{\rho cA}$	$\frac{B}{\rho cA}$	$\frac{G}{\rho cA}$	$\frac{B}{\rho cA}$	$\frac{G}{\rho cA}$	$\frac{B}{\rho cA}$	$\frac{G}{\rho cA}$	$\frac{B}{\rho cA}$	$\frac{G}{\rho cA}$	$\frac{B}{\rho cA}$	$\frac{G}{\rho cA}$	$\frac{B}{\rho cA}$
1	0.447	0.403	0.497	0.376	0.479	0.411	0.468	0.343	0.538	0.333	0.520	0.338	0.566	0.256
3	0.334	0.296	0.372	0.286	0.361	0.346	0.360	0.319	0.434	0.360	0.418	0.406	0.477	0.385
5	0.453	0.361	0.446	0.354	0.443	0.338	0.433	0.346	0.409	0.356	0.405	0.367	0.414	0.399
7	0.400	0.296	0.416	0.304	0.432	0.325	0.431	0.327	0.446	0.324	0.462	0.358	0.455	0.407
9	0.496	0.311	0.471	0.301	0.449	0.289	0.467	0.294	0.500	0.326	0.512	0.347	0.520	0.351
11	0.420	0.296	0.442	0.297	0.480	0.306	0.484	0.326	0.472	0.348	0.491	0.368	0.544	0.397
13	0.496	0.311	0.478	0.325	0.451	0.342	0.452	0.340	0.467	0.325	0.479	0.340	0.499	0.393
15	0.400	0.296	0.413	0.285	0.428	0.262	0.444	0.265	0.484	0.284	0.521	0.292	0.538	0.319
17	0.453	0.361	0.441	0.355	0.429	0.350	0.427	0.330	0.430	0.312	0.459	0.300	0.503	0.281
19	0.334	0.296	0.384	0.302	0.378	0.267	0.401	0.318	0.473	0.316	0.468	0.340	0.515	0.441
21	0.447	0.403	0.484	0.427	0.453	0.368	0.422	0.435	0.444	0.433	0.393	0.430	0.376	0.490
2	0.368	0.402	0.424	0.367	0.427	0.409	0.428	0.355	0.511	0.389	0.456	0.423	0.486	0.368
4	0.301	0.353	0.341	0.349	0.323	0.403	0.325	0.381	0.370	0.427	0.347	0.446	0.396	0.432
6	0.362	0.325	0.356	0.316	0.356	0.308	0.355	0.326	0.353	0.343	0.378	0.374	0.389	0.434
8	0.392	0.267	0.415	0.278	0.438	0.295	0.456	0.275	0.481	0.255	0.471	0.272	0.434	0.282
10	0.402	0.238	0.386	0.237	0.374	0.245	0.387	0.280	0.395	0.324	0.399	0.327	0.420	0.303
12	0.389	0.258	0.406	0.259	0.424	0.260	0.400	0.259	0.367	0.258	0.377	0.266	0.427	0.292
14	0.402	0.238	0.387	0.243	0.372	0.252	0.394	0.250	0.437	0.239	0.462	0.265	0.455	0.331
16	0.392	0.267	0.408	0.265	0.435	0.254	0.429	0.282	0.413	0.343	0.398	0.374	0.372	0.367
18	0.362	0.325	0.348	0.340	0.337	0.368	0.335	0.376	0.319	0.378	0.317	0.394	0.335	0.404
20	0.301	0.353	0.353	0.360	0.341	0.305	0.342	0.347	0.403	0.334	0.381	0.336	0.405	0.397
22	0.368	0.402	0.393	0.429	0.368	0.414	0.352	0.459	0.376	0.464	0.349	0.466	0.349	0.509

Figures 6a through 6g are the directivity patterns for angles of steering of the major lobe from 0 degree through 30 degrees in 5 degree steps. In every case the same voltage magnitude of 300 volts is applied to each unit and the necessary phases of voltage required to produce the indicated beam steering is determined for the no-interaction case. These patterns are the patterns obtained by rotating the array about a vertical axis (an axis normal to the long dimension of the array lying in the plane of the array). All patterns are computed using the normalization factor for the 0-degree no-interaction pattern.
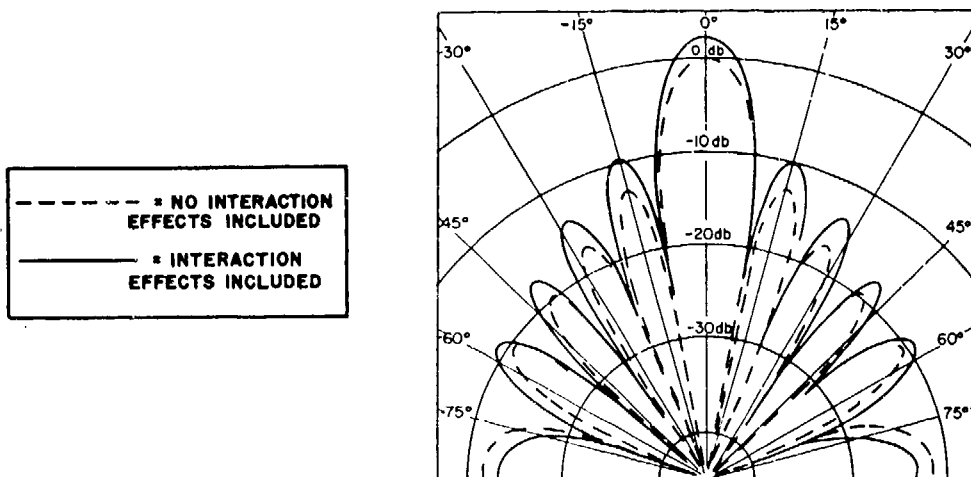
(a) Main lobe steered 0 degrees
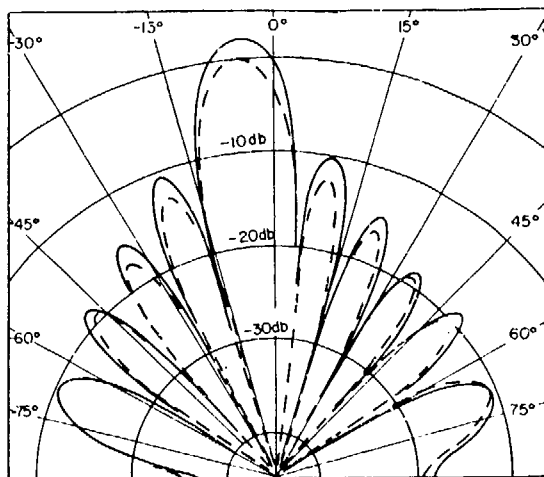
(b) Main lobe steered 5 degrees   (c) Main lobe steered 10 degrees

Fig. 6 - Directivity patterns in the horizontal plane of the XEM-3B array. All units are driven with equal voltage magnitude and in phase.
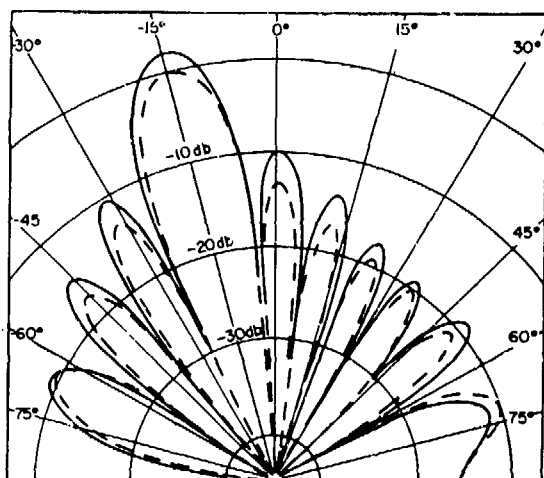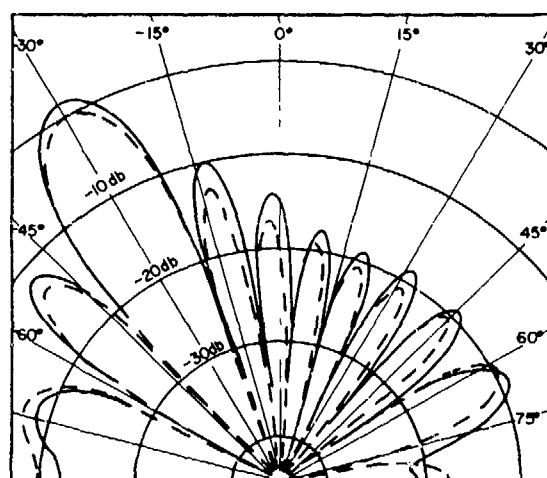
(d) Main lobe steered 15 degrees
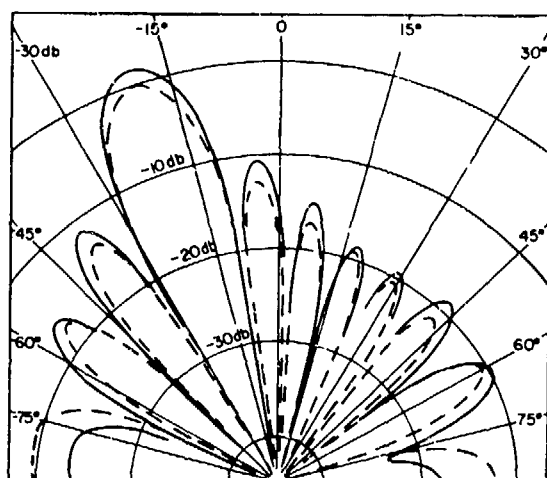
(e) Main lobe steered 20 degrees
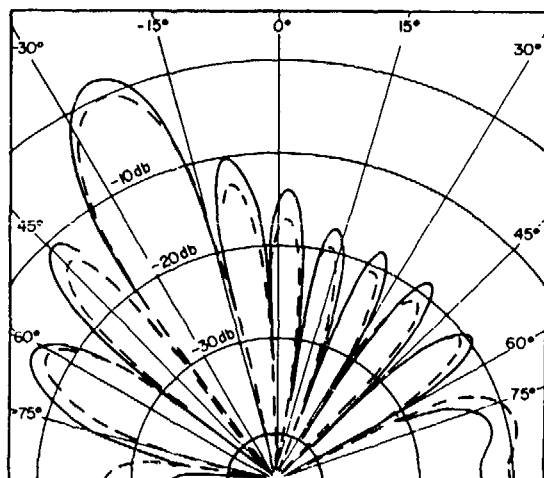
(f) Main lobe steered 25 degrees

(g) Main lobe steered 30 degrees

Fig. 6 (Continued) - Directivity patterns in the horizontal plane of the XEM-3B array. All units are driven with equal voltage magnitude and in phase.

In the 0-degree pattern, the major lobe height or effective source level has been increased about 2.2 db with respect to the no-interaction pattern for the same excitation conditions. It is noted further that the gain in principal lobe height or effective source level has been reduced to only about 1.5 db (as compared with the no-interaction pattern) when the main lobe is steered 30 degrees away from broadside. When proper account is taken of the difference in level on the acoustic (0-degree) axis, then as the point of observation is varied from 0 to 90 degrees, the side lobes for the interaction pattern are seen to be larger than the no-interaction side lobes near the principal lobe, but the difference

gradually diminishes and the side lobes become less than the corresponding side lobes of the no-interaction pattern beyond about 40 degrees for the unsteered situation. In addition to the changes in lobe heights, the nulls between the lobes are filled in, some rotation of the side lobes has occurred, and some increase in the beamwidth occurs.

Table 3 gives values for the total input impedance for each radiator as a function of beam steering. Generally in this table the real part of the input impedance decreases with beam steering. The inner radiators usually have the smaller reactive component of impedance whereas the real part of the input impedance tends to be smaller for the outside radiators.

Table 3
Input Impedance of Each Radiation as a
Function of the Angle of Steering of the Main Lobe
Zinput = R + jX (ohms)

Rad. No.	0°		5°		10°		15°		20°		25°		30°	
	R	X	R	X	R	X	R	X	R	X	R	X	R	X
1	119.3	176.9	118.5	185.7	115.7	180.6	125.3	185.2	119.3	194.2	120.6	191.9	123.0	205.3
3	149.4	169.1	145.6	177.7	136.3	168.2	141.4	171.1	126.4	178.8	120.9	172.5	119.2	182.4
5	124.4	181.5	126.2	181.2	128.8	182.4	128.6	180.1	129.6	175.5	128.2	173.8	122.3	172.5
7	140.1	181.0	136.8	182.5	131.8	182.3	131.6	181.9	130.2	184.4	124.0	182.9	118.1	177.8
9	126.2	192.1	130.2	190.4	134.6	189.1	131.6	190.8	124.0	190.9	120.5	190.1	119.2	190.5
11	137.4	184.2	134.4	187.2	128.6	190.8	125.7	189.0	124.3	185.2	119.9	185.7	112.3	189.1
13	126.2	192.1	126.6	188.4	127.3	183.1	127.4	183.5	127.7	187.0	124.6	187.0	116.2	184.4
15	140.1	181.0	140.1	184.6	141.0	190.2	138.3	191.8	130.7	194.1	125.3	197.0	120.7	195.6
17	124.4	181.5	126.6	180.4	128.5	179.2	131.5	181.0	133.8	183.5	131.9	189.1	128.6	196.4
19	149.4	169.1	141.3	177.7	148.2	181.8	136.6	178.3	128.1	188.8	125.7	185.5	109.7	182.7
21	119.3	176.9	113.4	180.0	120.9	179.0	116.4	171.1	115.3	174.4	118.9	166.9	110.2	161.5
2	125.3	164.7	126.4	176.7	119.9	173.6	127.7	178.5	115.8	186.2	115.9	176.7	120.5	185.0
4	140.7	155.1	137.7	163.9	128.2	156.0	132.4	157.9	120.8	163.4	118.8	158.3	118.5	167.4
6	139.9	170.7	142.6	170.7	144.0	171.7	140.5	169.3	137.5	167.0	129.4	168.5	118.6	166.2
8	145.9	184.0	140.8	185.9	135.3	186.9	135.4	191.9	134.3	197.6	133.8	194.1	137.5	188.1
10	148.9	190.4	151.8	188.1	152.6	184.8	144.6	181.3	136.2	176.8	135.3	177.0	136.5	183.1
12	147.9	185.0	145.0	187.6	141.9	189.9	146.0	186.6	151.5	181.3	148.6	181.8	137.1	185.7
14	148.9	190.4	150.6	187.3	151.7	183.2	148.5	187.1	142.8	194.8	135.8	194.1	128.3	184.9
16	145.9	184.0	143.7	187.1	141.0	192.3	138.3	187.4	131.1	177.5	127.7	172.0	131.1	168.2
18	139.9	170.7	138.7	166.3	134.1	161.4	132.8	160.4	133.6	157.0	130.3	155.4	127.1	158.3
20	140.7	155.1	134.4	165.3	146.6	169.3	137.9	164.5	133.6	176.9	136.8	173.5	123.3	171.1
22	125.3	164.7	119.1	167.0	123.2	163.7	116.2	158.7	114.3	162.4	115.1	157.9	107.9	156.7

Table 4 gives values for the real and imaginary part of the input impedance for each vertical stave of the array as a function of the beam steering. The information in Table 4 is a combination of the results from Table 3 and is of principal interest to the transmitter designer who wonders what happens to impedance vs lobe steering.

Table 4
Input Impedance for Vertical Staves as a Function of the Steering of the Main Lobe
Z_p (staves) $= R_p + jX_p$ (ohms)

Stave* No.	Rad. Nos.	0°		5°		10°		15°		20°		25°		30°	
		R_p	X_p	R_p	X_p	R_p	X_p	R_p	X_p	R_p	X_p	R_p	X_p	R_p	X_p
I	1 & 2	30.6	42.7	30.6	45.3	29.5	44.3	31.6	45.5	29.4	47.5	29.6	46.0	30.5	48.7
II	3 & 4	36.2	35.5	35.4	42.6	33.0	40.5	34.2	41.1	30.9	42.7	30.0	41.3	29.7	43.7
III	5 & 6	33.1	44.1	33.6	44.1	34.1	44.3	33.7	43.7	33.4	42.8	32.2	42.8	30.1	42.3
IV	7 & 8	35.7	45.6	34.7	46.0	33.4	46.1	33.4	46.7	33.1	47.7	32.2	47.1	31.8	45.7
V	9 & 10	34.3	47.9	35.2	47.4	35.9	46.8	34.6	46.6	32.6	46.0	32.1	45.9	32.0	46.8
VI	11 & 12	35.6	46.2	34.9	46.9	33.8	47.6	33.9	47.1	34.4	46.0	33.5	46.1	31.1	47.0
VII	13 & 14	34.3	47.9	34.6	47.1	34.8	45.9	34.4	46.4	33.7	47.7	32.5	47.6	30.5	46.2
VIII	15 & 16	35.7	45.6	35.5	46.5	35.3	47.8	34.6	47.4	32.8	46.4	31.7	46.0	31.7	45.4
IX	17 & 18	33.1	44.1	33.2	43.4	32.9	42.5	33.1	42.6	33.5	42.4	32.9	42.8	32.2	44.0
X	19 & 20	36.2	40.5	34.4	42.8	36.9	43.9	34.4	42.8	32.8	45.7	32.9	44.9	29.2	44.3
XI	21 & 22	30.6	42.7	29.1	43.4	30.6	42.8	29.1	41.2	28.7	42.1	29.2	40.6	27.3	39.5
	Av	34.1	43.9	33.7	45.0	33.7	44.8	33.4	44.6	32.3	45.2	31.7	44.6	30.6	4..9

*The four radiators in each stave are in parallel.

Table 5 gives values for the real power into each radiator and the real power out of each radiator as a function of beam steering when the excitation voltage has a magnitude of 300 volts. For each situation of beam steering the power into and out of the radiators is greater for the inner radiators with the exception of 7 and 8. The power into and out of the array generally decreases when the major lobe is steered away from broadside.

Table 6 gives values of the efficiencies of the radiators as a function of beam steering. The efficiency for each situation of beam steering is generally better for the outer radiators with the exception of radiators 7 and 8. The conversion efficiency increases slightly with beam steering.

CONCLUSIONS

In conclusion, some of the more interesting results which have been noted from the inclusion of the interaction effects into a large low-frequency array are summarized. This array has rather large inactive areas associated with it and in this respect the interactions are rather small.

The outer radiators of the array have the greater real part of the radiation load, the smaller velocities, and the better efficiencies. This is in general agreement with Mr. Stickley's report* on velocity zones in an array.

---

*A.R. Stickley, "Behavior of the Response Pattern of a Circularly Zoned Plane Array with Variation of the Zone Boundaries," U.S. Navy Journal of Underwater Acoustics 1 (No. 1): 58-68 (1951) (Confidential)

Table 5
Real Power In and Real Power Out as a Function of the Angle of Steering
of the Main Lobe (watts for 300 volts excitation)

Rad. No.	0°		5°		10°		15°		20°		25°		30°	
	In	Out	In	Out	In	Out	In	Out	In	Out	In	Out	In	Out
1	235.8	140.5	219.8	136.1	226.4	137.2	225.6	139.0	206.7	132.1	211.3	133.8	193.3	127.4
3	264.1	149.7	248.2	146.2	261.8	149.1	258.3	148.7	237.3	142.4	245.2	143.1	226.0	138.0
5	231.3	140.4	233.0	141.2	232.5	141.4	236.3	142.4	245.1	144.8	247.4	145.1	246.2	143.7
7	240.7	144.4	236.6	143.1	234.4	142.3	235.0	142.3	230.0	140.8	228.5	139.6	233.3	139.6
9	215.0	135.8	220.3	137.8	224.8	139.5	220.5	138.0	215.3	135.6	214.2	134.7	212.4	133.9
11	234.3	142.5	227.8	140.4	218.6	137.1	219 5	137.2	224.8	138.6	220.9	136.7	209.0	131.3
13	215.0	135.8	221.1	137.8	230.3	140.7	229.8	140.5	224.1	138.8	222.1	137.8	220.1	135.7
15	240.7	144.4	234.8	142.7	226.4	140.0	222.6	138.8	214.8	136.1	206.9	132.9	205.6	131.9
17	231.3	140.4	234.6	141.7	237.8	142.8	236.4	142.8	233.4	142.1	223.4	138.9	210.0	134.2
19	264.1	149.7	246.8	145.9	242.4	144.0	243.6	145.0	221.4	138.1	225.3	138.9	215.4	132.8
21	235.8	140.5	225.5	136.2	233.3	140.3	244.6	141.6	237.5	139.7	254.9	144.4	259.4	141.2
2	263.4	147.7	241.0	143.3	242.3	142.2	238.7	142.9	216.8	134.6	233.6	139.0	223.5	137.2
4	288.8	153.7	270.4	150.9	283.0	151.3	280.6	151.8	263.4	146.5	272.9	147.0	253.5	144.0
6	258.4	148.7	259.5	148.9	258.1	148.6	261.2	149.2	264.4	149.7	258.0	147.6	256.1	144.5
8	238.1	143.4	233.0	142.1	228.7	140.7	221.0	138.3	211.8	135.0	216.7	136.7	228.9	140.6
10	229.4	140.5	233.9	141.6	239.2	143.1	242.0	144.6	246.1	145.6	245.4	145.4	235.5	142.8
12	237.3	143.0	232.2	141.7	227.2	140.3	234.2	142.2	244.3	144.7	242.6	144.5	231.6	141.7
14	229.4	140.5	234.7	142.0	241.3	143.9	234.2	142.1	220.3	137.8	217.8	137.2	228.0	140.1
16	238.1	143.4	232.4	141.8	223.2	139.0	229.5	141.0	242.3	144.3	250.4	145.7	259.5	148.2
18	258.4	148.7	266.2	150.2	274.1	151.1	275.6	151.2	283.0	152.3	285.1	152.0	277.6	150.3
20	288.8	153.7	266.4	149.9	263.1	149.2	269.4	150.7	244.7	145.1	252.2	147.1	249.4	144.5
22	263.4	147.8	254.7	144.4	264.2	147.3	270.4	145.6	260.9	143.5	271.3	145.2	268.3	140.7
Total*	5401.6	3175.2	5272.9	3145.9	5313.1	3151.1	5328.9	3156.0	5188.4	3108.2	5246.1	3113.3	5140.7	3064.3
Av*	245.5	144.3	239.7	143.0	241.5	143.2	242.2	143.5	235.8	141.3	238.5	141.5	233.7	139.3

*One-half of the array

Table 6
Radiator Efficiency (percent) as a Function
of the Angle of Steering of the Main Lobe

Rad. No.	0°	5°	10°	15°	20°	25°	30°
1	59.6	61.9	60.6	61.6	63.9	63.3	65.3
3	56.7	58.9	57.0	57.5	60.0	58.4	61.1
5	60.7	60.6	60.8	60.3	59.1	58.7	58.4
7	60.0	60.5	60.7	60.6	61.2	61.1	59.8
9	63.1	62.5	62.1	62.0	63.0	62.9	63.0
11	60.8	61.6	62.7	62.5	61.6	61.9	62.9
13	63.1	62.3	61.1	61.1	62.0	62.1	61.6
15	60.0	60.8	61.8	62.4	63.3	64.2	64.2
17	60.7	60.4	60.1	60.4	60.9	62.2	63.9
19	56.7	59.1	59.4	59.5	62.3	61.7	61.7
21	59.6	60.4	60.2	57.9	58.8	56.7	54.4
2	56.1	59.5	58.7	59.6	62.1	59.5	61.7
4	53.2	55.8	53.5	54.1	55.6	53.9	56.8
6	57.5	57.4	57.6	54.1	56.6	57.2	56.4
8	60.2	61.0	61.5	62.3	63.8	63.1	61.7
10	61.3	60.6	60.0	59.8	59.1	59.2	60.7
12	60.3	61.0	61.7	60.7	59.2	59.6	61.2
14	61.3	60.5	59.6	60.7	62.6	63.0	61.4
16	60.2	61.0	62.3	61.4	59.6	58.2	57.1
18	57.5	56.4	55.1	54.8	53.8	53.3	54.1
20	53.2	56.2	56.7	55.9	59.3	58.3	57.9
22	56.1	56.7	55.8	55.8	55.0	53.5	52.4
Av	58.8	59.7	59.3	59.2	59.9	59.4	59.9

The behavior of the individual radiators in the array as the major lobe is steered away from the broadside position reveals a decreases in the velocities, an increase in the radiation load, and a small gain in the conversion efficiency.

For the array as a whole, both the power into and the power out of the array decrease but the conversion efficiency (as determined from the ratio of the total acoustic power delivered by the array to the total electrical power into the array) increases as the major lobe is steered away from the principal axis of the array. The effective source level of the array is reduced as the major lobe is steered.

The fact that the array is more efficient (minimum value 58.8 percent) when the interactions are included as compared with 55.8 percent for the situation which neglects interactions completely has not been explained thus far.

Additional situations which take into account the effects of nonidentical elements are being computed and will be reported at a later date. The element variations which are presently being investigated are the resonant frequency and the mechanical Q in air.

The method will also permit the investigation of effects of variation in the electro-mechanical force factor, electromechanical coupling coefficient, position variation of the foregoing primary variations, electrical tuning networks, and array shading without additional mathematical complication other than handling large numbers of computations.

ACKNOWLEDGMENTS

Appendix A

DEFINITIONS OF SYMBOLS

Y_{m_n} = Mutual acoustic immobility in gm per sec between unit m and the radiator n computed in accordance with Eq. C-30, p. 148, of Pritchard's "Directivity of Acoustic Linear Point Arrays."

Y_{11} = Radiation self-immobility for the element in gm per sec.

Y_s = $G_s + j\ B_s$

G_s = Mechanical unresponsiveness* for the element in air = 0.1326×10^7 gm/sec.

B_s = $\dfrac{-1}{\omega C_s}$ = Unexcitability for the element in gm per sec* = -4.83×10^7 gm/sec.

ω = $2\pi F$ = Angular frequency in radians per sec = $2\pi \times 10^3$.

C_s = Compliance of the element.

Y_{m_1} = $j\omega m_1$ = j 6.85×10^7 gm/sec.

Y_{m_2} = $j\omega m_2$ = j 16.34×10^7 gm/sec.

V_{i_n} = The velocity of the nonradiating mass (m_1) in cm per sec for the nth radiator.

V_n = The velocity of the radiating mass (m_2) in cm per sec for the nth radiator.

V_{ni} = The velocity across the secondary of the "transformer" in cm per sec for the nth radiator.

f_n = Force developed across the "secondary of the transformer" by the current i flowing in the primary for the nth radiator.

f_{on} = Force due to any external acoustic sources other than those included in the interactions for the nth radiator.

F' = Voltage in abvolts (1 volt = 10^8 abvolts) applied to a single element.

E_{pn} = Voltage across the primary of the transformer for a single element.

E = Voltage applied to four elements in series electrically = 3×10^{10} abvolts.

i_n = Current in the primary circuit of nth element.

T = Turns ratio in dynes per abamp for the transformer in the mobility analogy circuit for the element = 4.18×10^8 dynes/abamp.

---

*See F.A. Firestone, "Twixt Earth and Sky with Rod and Tube," J. Acoust. Soc. Amer. 28:1126 (1956)

Z_c = Clamped impedance for the element transducer

$$= (3 + j\ 56) \times 10^9 \text{ abohms}$$

$$= (3 + j\ 66) \text{ ohms}$$

CONFIDENTIAL

Naval Research Laboratory. Report 5251 [CONFIDENTIAL].
EVALUATION OF EFFECTS OF ELEMENT INTERACTIONS IN A LARGE-LOW
FREQUENCY ARRAY [unclassified Title], by Roland V. Baier.
21 pp. & Figs. February 10, 1959.

Mutual interactions between elements of a transducer array
affect the velocities, radiation loading, and beam patterns which
are obtained in a given array and unit design. These effects are
of particular interest for transducer arrays which have relatively
large inactive areas interspersed in the radiating surface. These
interaction effects have been evaluated from theoretical expres-
sions in a manner which takes account of the array geometry, the
electromechanical properties of the array elements, and the phase
and magnitude of the electrical excitation of a 84-unit 1-kc
planar array.

The results of the computations are presented as the
theoretical velocities, radiation loading, input impedance, power
in, power out, and the efficiencies which are effective for the
individual elements in the array within the assumptions made in
the theory. These results are presented for several degrees of

CONFIDENTIAL   (Over)

1. Sonar projectors -
   Interactions

I. Baier, R.V.

CONFIDENTIAL

Naval Research Laboratory. Report 5251 [CONFIDENTIAL].
EVALUATION OF EFFECTS OF ELEMENT INTERACTIONS IN A LARGE-LOW
FREQUENCY ARRAY [unclassified Title], by Roland V. Baier.
21 pp. & Figs. February 10, 1959.

Mutual interactions between elements of a transducer array
affect the velocities, radiation loading, and beam patterns which
are obtained in a given array and unit design. These effects are
of particular interest for transducer arrays which have relatively
large inactive areas interspersed in the radiating surface. These
interaction effects have been evaluated from theoretical expres-
sions in a manner which takes account of the array geometry, the
electromechanical properties of the array elements, and the phase
and magnitude of the electrical excitation of a 84-unit 1-kc
planar array.

The results of the computations are presented as the
theoretical velocities, radiation loading, input impedance, power
in, power out, and the efficiencies which are effective for the
individual elements in the array within the assumptions made in
the theory. These results are presented for several degrees of

CONFIDENTIAL   (Over)

1. Sonar projectors -
   Interactions

I. Baier, R.V.

CONFIDENTIAL

Naval Research Laboratory. Report 5251 [CONFIDENTIAL].
EVALUATION OF EFFECTS OF ELEMENT INTERACTIONS IN A LARGE-LOW
FREQUENCY ARRAY [unclassified Title], by Roland V. Baier.
21 pp. & Figs. February 10, 1959.

Mutual interactions between elements of a transducer array
affect the velocities, radiation loading, and beam patterns which
are obtained in a given array and unit design. These effects are
of particular interest for transducer arrays which have relatively
large inactive areas interspersed in the radiating surface. These
interaction effects have been evaluated from theoretical expres-
sions in a manner which takes account of the array geometry, the
electromechanical properties of the array elements, and the phase
and magnitude of the electrical excitation of a 84-unit 1-kc
planar array.

The results of the computations are presented as the
theoretical velocities, radiation loading, input impedance, power
in, power out, and the efficiencies which are effective for the
individual elements in the array within the assumptions made in
the theory. These results are presented for several degrees of

CONFIDENTIAL   (Over)

1. Sonar projectors -
   Interactions

I. Baier, R.V.

CONFIDENTIAL

Naval Research Laboratory. Report 5251 [CONFIDENTIAL].
EVALUATION OF EFFECTS OF ELEMENT INTERACTIONS IN A LARGE-LOW
FREQUENCY ARRAY [unclassified Title], by Roland V. Baier.
21 pp. & Figs. February 10, 1959.

Mutual interactions between elements of a transducer array
affect the velocities, radiation loading, and beam patterns which
are obtained in a given array and unit design. These effects are
of particular interest for transducer arrays which have relatively
large inactive areas interspersed in the radiating surface. These
interaction effects have been evaluated from theoretical expres-
sions in a manner which takes account of the array geometry, the
electromechanical properties of the array elements, and the phase
and magnitude of the electrical excitation of a 84-unit 1-kc
planar array.

The results of the computations are presented as the
theoretical velocities, radiation loading, input impedance, power
in, power out, and the efficiencies which are effective for the
individual elements in the array within the assumptions made in
the theory. These results are presented for several degrees of

CONFIDENTIAL   (Over)

1. Sonar projectors -
   Interactions

I. Baier, R.V.

CONFIDENTIAL

electrically steering of the principal lobe. Plots of the patterns are presented for various amounts of electrical steering of the principal lobe and are compared with the situation which would result if the interaction effects were neglected.

Some of the more interesting observations are the following. The outer radiators of the array have the greater real part of the radiation load, the smaller velocities, and the better efficiencies. The behavior of the individual radiators in the array as the major lobe is steered away from the broadside position reveals a decrease in the velocities, an increase in the radiation load, and a small gain in the conversion efficiency. For the array as a whole, both the power into and the power out of the array decrease but the conversion efficiency (as determined from the ratio of the total acoustic power delivered by the array to the total electrical power into the array) increases as the major lobe is steered away from the principal axis of the array. The effective source level of the array is reduced as the major lobe is steered. The fact that the array is more efficient (minimum value 58.8 percent) when the interactions are included as compared with 55.8-percent efficiency when interactions are neglected completely has not been explained thus far. [Confidential Abstract]

CONFIDENTIAL

7103/136

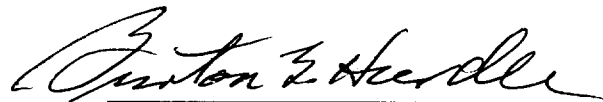DATE: 19 November 1996

FROM: Burton G. Hurdle (Code 7103)

SUBJECT: REVIEW OF REF. (a) FOR DECLASSIFICATION

TO: Code 1221.1

VIA: Code 7100

AD- 305 684

REF: (a) NRL Confidential Report #5251 by Roland V. Baier, 10 Feb 1959 (U)

1. Reference (a) is a report of theoretical studies of the effects of element interaction in a large 1-kc planar array.

2. This technology is well known today.

3. Based on the above, it is recommended that reference (a) be declassified and released with no restrictions.

BURTON G. HURDLE
Acoustics Division

CONCUR:

EDWARD R. FRANCHI   11/20/96
Superintendent   Date
Acoustics Division

completed
1-24-2000
B.W.

OPTIONAL FORM NO. 19
(REV). 1-80)
GSA FPMR(41 CFR) 101-11.6
5010-114